Mon. Not. R. Astron. Soc. **000**, 1–5 (2011) Printed 20 September 2011 (MN LATEX style file v2.2)

Statistical Mechanics of 1d Self-Gravitating Systems: The Core-Halo Distribution

T. N. Teles[1⋆], Y. Levin[1]† and R. Pakter[1]‡

[1] *Instituto de Física, Av. Bento Gonçalves, 9500, Caixa Postal 15051, 91501-970 - Porto Alegre, RS, Brazil*

arXiv:1109.3780v1 [astro-ph.GA] 17 Sep 2011

ABSTRACT

We study, using both theory and simulations, a system of self-gravitating sheets. A new statistical mechanics theory — free of any adjustable parameters — is derived to quantitatively predict the final stationary state achieved by this system after the process of collisionless relaxation is complete. The theory shows a very good agreement with the numerical simulations. The model sheds new light on the general mechanism of relaxation of self-gravitating systems and may help us to understand cold matter distribution in the universe.

Key words: Gravitation – Globular Clusters – Galaxies: Statistics

1 INTRODUCTION

One of the most fundamental questions of astrophysics concerns the mass distribution after a self-gravitating system has relaxed to equilibrium. This problem, posed more than 6 decades ago, still remains unresolved, see the recent papers (Hjorth & Williams 2010; Barnes & Williams 2011) and references therein. In the astrophysical context, the answer to this question may help to shed light on a lot of intriguing theoretical puzzles, such as the physical mechanism responsible for the regularities observed in the light profile of elliptical galaxies and the mass distribution in the dark matter halos.

The classical simulations of Navarro, Frenk & White (1995, 1996, 1997) have produced the density profiles of dark matter halos that no present theory is capable of explaining, see (Camm 1950; Hohl & Feix 1966; Lynden-Bell 1967; Hohl & Campbell 1968; Cuperman, Goldstein & Lecar 1969; Shu 1978; White & Narayan 1987; Saslaw 2000) and references therein. The scope of the problem extends from the foundations of statistical mechanics to the large scale evolution of the universe, (Padmanabhan 1990). The purpose of the present paper is to construct a statistical theory that is able to successfully predict both the mass and the velocity distributions of a self-gravitating system after it has completed the process of collisionless relaxation. In this respect the One Dimensional Self-Gravitating Model (ODSGM) of interacting mass sheets, has proven very useful for understanding both the stellar dynamics and the cosmological models, see (Wright, Miller & Stein 1982; Mathur 1990; Joyce & Worrakitpoonpon 2010a,b; Miller & Rouet 2010; Joyce & Sicard 2011) and references therein. Although much simpler than the real three dimensional gravity, this model contains the essence of the gravitational problem: long-range potential (Campa, Dauxois & Ruffo 2009) and collective motion damped by particle-wave interactions which leads to collisionless relaxation, (Levin, Pakter & Teles 2008a; Levin, Pakter & Rizzato 2008b; Teles et al. 2010; Pakter & Levin 2011) and references therein. The ODSGM is particularly convenient because the sheet-sheet interaction potential is not singular, so that the model can be easily simulated (Noullez, Fanelli & Aurell 2003). At the same time it contains much of the same complicated statistical mechanics (Campa et al. 2009) of other systems with long-range forces: broken ergodicity and lack of mixing, which also plague gravity in three dimensions.

Long before the empirical works of Navarro et al. (1995, 1996, 1997) Lynden-Bell (LB) proposed a statistical theory of self-gravitating systems based on the Vlasov equation (Lynden-Bell 1967). The LB theory has become known as the Theory of Violent Relaxation. One of the fundamental assumptions of LB was that violent relaxation leads to an efficient phase-space mixing. The subsequent simulations, however, have shown that this is not the case (Bindoni & Secco 2007; Yamaguchi 2008; Levin et al. 2008a,b; Teles et al. 2010; Navarro et al. 2010). Therefore, a new approach is needed if one wants to theoretically understand the structure of self-gravitating systems in equilibrium.

We will work in thermodynamic limit — the number of sheets N diverges, the mass of each sheet m goes to zero, while the total mass M of the system remains fixed, $mN = M$. The advantage of working with 1d system is that the gravitational potential is unbounded from above

⋆ E-mail: teles@if.ufrgs.br
† E-mail: levin@if.ufrgs.br
‡ E-mail:pakter@ufrgs.br

and bounded from below. As a consequence of this — after a sufficient large time $\tau_\times$, known as the Chandrasekhar time — a finite self-gravitating system must relax to the usual Maxwell-Boltzmann (MB) equilibrium (Rybicki 1971). In the limit $N \to \infty$, the Chandrasekhar time diverges and the system becomes trapped in an out-of-equilibrium stationary state (Wright et al. 1982; Reidl & Miller 1995; Tsuchiya & Gouda 1995, 1996, 2000; Yawn & Miller 2003; Teles et al. 2010; Gupta & Mukamel 2010). Although 3d self-gravitating systems never relax to MB equilibrium they also become trapped in a quasi-Stationary State qSS (Levin et al. 2008a,b). In fact, for real 3d self-gravitating systems, such as elliptical galaxies, the life time of the qSS is larger than their proper life span (Binney & Tremaine 2008). For ODSGM it has been observed that qSS state has a very long life-span even for a small number of particles (Wright et al. 1982).

This letter is organized as follows. In section 2 we introduce the 1d gravitational sheet model. In section 3 we comment briefly on its general dynamics and present the results of numerical simulation. In section 4 we derive the equation which is capable, over a short time span, to accurately describe the oscillations of the root-mean-square of particle positions. In section 5 we present the statistical-mechanics theory that is able to accurately predict both the velocity and the mass distribution in equilibrium, without any adjustable parameters. The more involved derivation of the envelope equation is left to the appendix of the paper, A.

2 THE MODEL'S DESCRIPTION

The ODSGM consists of N sheets of mass m_i in the $y-z$ plane, free to move along the x-axis. To simplify the calculations, we suppose that all the sheets have the same mass $m_i = m = M/N$, where M is the total mass of the system. The sheets interact through the one dimension gravitational potential that satisfies the Poisson equation

$$\nabla^2\psi(x,t) = 4\pi G\rho(x,t)\,, \tag{1}$$

where G is the gravitational constant and $\rho(x,t)$ is the mass density.

We define dimensionless variables by scaling mass, lengths, velocities, the potential, the mass density and the energy with respect to M, L_0 (an arbitrary length scale), $V_0 = \sqrt{2\pi GML_0}$, $\psi_0 = 2\pi GML_0$, $\rho_0 = M/2L_0$ and $E_0 = MV_0^2 = 2\pi GM^2L_0$, respectively. All these scales correspond to setting $G = M = 1$ and to defining the dynamical time scale as,

$$\tau_D = (4\pi G\rho_0)^{-1/2}. \tag{2}$$

It is then easy to show that a particle (sheet) at the origin with a mass density $\rho(x) = \delta(x)$ creates a long-range gravitational potential,

$$\psi(x) = |x|\,. \tag{3}$$

Systems with long-range interaction are very peculiar because in the thermodynamic limit the collision duration time diverges, and the dynamical evolution of the system is governed exactly by the collisionless Boltzmann (Vlasov) equation, (Braun & Hepp 1977)

$$\frac{Df}{D\mathrm{t}} = \frac{\partial f}{\partial \mathrm{t}} + \mathrm{v}\frac{\partial f}{\partial \mathrm{x}} - \nabla\psi(\mathrm{x},\mathrm{t})\frac{\partial f}{\partial \mathrm{v}} = 0, \tag{4}$$

where $f(\mathrm{x},\mathrm{v},\mathrm{t})$ is the one particle distribution function, so that $\rho(\mathrm{x},\mathrm{t}) = \int f(\mathrm{x},\mathrm{v},\mathrm{t})\mathrm{dv}$. Clearly real self-gravitating systems do not rigorously obey the $N \to \infty$ limit, nevertheless, in the astrophysical context the number of "particles" is usually very large, so that it constitutes a very good approximation.

The Vlasov equation has an infinite number of invariants called the Cassimirs (Chavanis 2006). Two of these are mass and energy,

$$\int \mathrm{dx}\,\mathrm{dv}\; f(\mathrm{x},\mathrm{v},\mathrm{t}) = 1\,, \tag{5}$$

$$\int \mathrm{dx}\,\mathrm{dv}\;\left(\frac{\mathrm{v}^2}{2} + \frac{\psi(\mathrm{x})}{2}\right)\; f(\mathrm{x},\mathrm{v},\mathrm{t}) = \mathcal{E}_0\,, \tag{6}$$

respectively, where $\mathcal{E}_0$ is the initial energy. Linear *momentum* is also a conserved quantity. However, by the symmetry of the problem and without loss of generality, it can be set to zero. In fact, any local functional of the distribution function is a Cassimir invariant of the Vlasov dynamics.

3 VLASOV DYNAMICS

Unlike collisional systems which after a very short time relax to the Maxwell-Boltzmann distribution, the time evolution of the Vlasov equation never ends. Instead it progresses to smaller and smaller length scales. In practice, however, both experiments and simulations have only a finite resolution. It is in this, coarse-grained, sense that we say that the Vlasov dynamics evolves to the stationary state. Unlike the usual MB equilibrium, however, the stationary state reached through the process of collisionless relaxation depends explicitly on the initial particle distribution.

3.1 Numerical Simulations

Numerical solution of the Vlasov equation is very complicated. One alternative is to perform directly the N-body simulation in which all particles evolve over time according to the usual Newton equations of motion (Noullez, Fanelli & Aurell 2003). We consider a ODSGM in which sheets are initially distributed in accordance with the water-bag distribution,

$$f_0(x,v) = \eta\Theta(x_m - |x|)\Theta(v_m - |v|) \tag{7}$$

where Θ is the Heaviside step function and $\eta = (4\; x_m v_m)^{-1}$ is the normalization constant obtained from Eq. (5). The values x_m and v_m are the limits of the distribution function in the phase space, so that without loss of generality we set $x_m = 1$. Due to the symmetry of the distribution, the total linear *momentum* is null and the only quantity other than the total mass to be conserved is the total energy $\mathcal{E}_0 = v_m^2/6 + 1/3$.

The halo formation is related to the initial condition through the only dimensionless parameter that remains after the rescaling of section 2 — the virial number, $\mathcal{R} = 2T/U$, where T is the total kinetic and U is the potential energy. When the virial condition $2T = U$ is not satisfied, $\mathcal{R} \neq 1$,

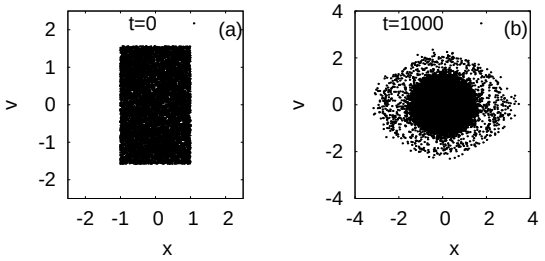

Figure 1. The initial (a) and final (b) phase space of 10^4 self-gravitating sheets initially distributed according to the water-bag distribution with the virial number $\mathcal{R}_0 = 2.5$.

the imbalance between the kinetic and the potential energies causes the system to develop collective oscillations which are then damped by particle-wave interactions, leading to the core-halo phase separation, Fig.1. Our interest in studying the distributions with $\mathcal{R} \neq 1$ arises from the fact that there is not even a qualitative theory that is able to account for the mass and velocity distributions for such systems (Yamashiro, Gouda & Sakagami 1992).

4 THE TEST PARTICLE MODEL

Systems with long-range forces display collective motion such as Langmuir waves in plasmas or Jeans waves in gravitational systems, Binney & Tremaine (2008). Since there are no collisions, interaction of individual particles with the density waves is the mechanism that responsible for the transfer of energy. The particle-wave interaction dampens the density waves while at the same time transfers large amounts of energy to the individual particles. The interaction is similar to a surfer "catching" a wave — some particles can gain a large amount of energy from the bulk oscillations to escape from the gravitational cluster and move to high energy regions of the phase space. These particles will then form a tenuous halo that will surround the dense low-energy core.

To study the oscillation of the initial gravitational cluster, we define the *envelope* as $x_e(t) \equiv \sqrt{3 < x(t)^2 >}$. Note that with this definition, at $t = 0$ the envelope is exactly the same as the extent of the initial particle distribution $x_e(0) = x_m$. For sufficiently short times, most particles will still remain within the limits set by $x_e(t)$. Differentiating $x_e(t)$ twice with respect to time, we find an approximate dynamical equation satisfied by $x_e(t)$,

$$\ddot{x}_e(t) = \frac{\mathcal{R}_0}{x_e(t)} - 1 \tag{8}$$

where $\mathcal{R}_0$ is the virial number of the initial distribution (the derivation is presented in Appendix A). We shall call this the "envelope equation" (Wangler et al. 1998; Davidson & Quin 2001). Equation 8 enables us to study the dynamics of a test particle x_i, subject to the oscillating potential produced by a uniform density distribution delimited by $-x_e(t) \leqslant x \leqslant x_e(t)$. A test particle moving in this potential will then evolve according to

$$\ddot{x}_i(t) = \begin{cases} -\frac{x_i(t)}{x_e(t)} \text{ for } |x_i(t)| \leqslant x_e(t) \\ -\text{sgn}[x_i(t) - x_e(t)] \text{ for } |x_i(t)| \geqslant x_e(t) \end{cases} \tag{9}$$

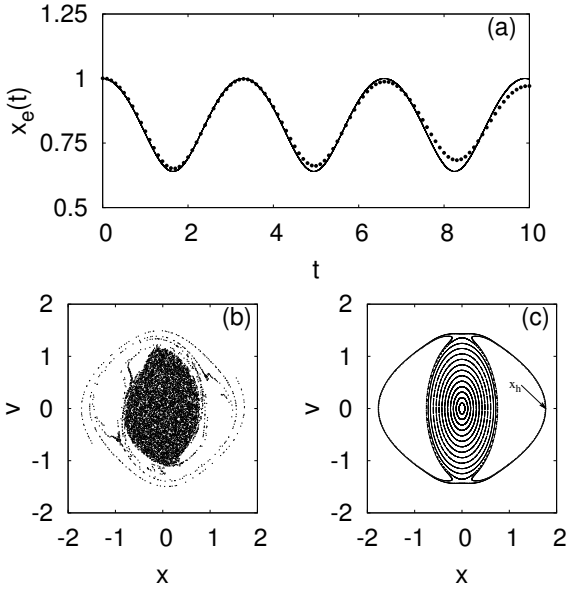

Figure 2. Test particle dynamics as compared to the N-body dynamics simulation: (a) corresponds to the evolution of $x_e(t)$ obtained from the N-body simulation (dots) while the solid line is calculated using the envelope equation. The time is in units of τ_D. (b) Represents the phase space after the first few oscillations and (c) is the Poincaré plot of the phase space produced by the test particles. Note the appearance of the resonance islands both in the N-body and test particle simulation. The test particle model allows us to accurately calculate the location of the resonant orbit with the maximum extent x_h. This will determine the maximum energy attained by the halo particles. At $t = 0$, 15 test particles were uniformly distributed from the center to slightly beyond the maximum core radius x_m with initial velocity 0.

where $x_e(t)$ is given by Eq. (8) and *sgn* is the sign function. In Fig. 2 we compare the complete N-body simulation with the test particle trajectories obtained from the numerical solution of Eqs. (8) and (9). The good agreement between the two reveals that for short times the envelope equation 8 is very accurate for describing the initial oscillations of the ODSGM. The formation of halo also occurs on a very short time scale — few oscillations of the envelope. Indeed, from Figs. 2 (b), (c), we see that the test particle model allows us to accurately locate the resonant orbits (Gluckstern 1994), which also delimit the extent of the halo in the full N-body simulations. Thus, the test particle model allows us to calculate the maximum energy — corresponding to the resonant orbit — attained by any of the halo particles. This energy will be used in the next Section to construct the core-halo distribution function.

5 THE CORE-HALO STATISTICAL THEORY

The Jeans theorem states that "any steady-state solution of the collisionless Boltzmann equation depends on the phase-space coordinates only through integrals of motion of the given potential, and any function of the integrals yields a steady-state solution of the collisionless Boltzmann equation", (Binney & Tremaine 2008). Thus, any function of energy is a solution to the Vlasov equation. In particular, the

Maxwell-Boltzmann distribution (MB) is also a stationary solution of the Vlasov equation. However, it is important to remember that MB is not a global attractor of the Vlasov dynamics — an arbitrary initial distribution of particles will not converge to the MB distribution, as happens for systems governed by short-range forces. In this paper we are interested in calculating the distribution to which the system will evolve, starting from an arbitrary water-bag-like initial condition, after the process of collisionless relaxation is completed.

We first observe that the Vlasov equation can be interpreted as a convective derivative of density over the phase-space, so that the distribution function evolves as an incompressible fluid. In the case of initial water-bag distribution this means that the phase-space density cannot exceed that of f_0, $f(\mathrm{x},\mathrm{v},\mathrm{t}) \leqslant \eta$. The mechanism of core-halo phase separation now becomes clear. Some particles enter in resonance with the rms bulk oscillations. They gain a lot of energy and escape from the main cluster, forming a tenuous halo. At the same time, evaporation of highly energetic particles dampens the core oscillations. This is similar to the process of evaporative cooling. The oscillations will stop when all of the free energy is exhausted. However, because of the constraint on the maximum density imposed by the Vlasov dynamics, the system cannot freeze — collapse to the minimum of the potential energy. Instead, the particle distribution of the core approaches that of a fully degenerate Fermi gas. With this physical insight in mind, we now propose an *ansatz* solution to the Vlasov equation:

$$f_{ch}(\mathrm{x},\mathrm{v}) \quad = \quad \eta\Theta\left[\epsilon_F - \epsilon\right] + \chi\Theta\left[\epsilon_h - \epsilon\right]\Theta\left[\epsilon - \epsilon_F\right] \qquad (10)$$

where ϵ_F is the Fermi energy, ϵ_h is the halo (resonance) energy, and $\epsilon(x,v) = v^2/2 + \psi(x)$ is the one particle energy. The halo energy is obtained simply by taking the most extended position of test particle x_h when it crosses the $v = 0$ axis, in others words $\epsilon_h = |x_h|$. The Fermi energy, ϵ_F, delimits the extent of the core region, and χ measures the phase space density inside the halo. Both of these parameters are calculated self-consistently from the norm and energy conservation equations, Eqs. (5) and (6).

Substituting Eq. 10 into the Poisson equation and integrating the core-halo distribution function over velocity, the dimensionless Poisson equation becomes

$$\frac{d^2\psi}{d\mathrm{x}^2} = 2\sqrt{2}\begin{cases} (\eta-\chi)\sqrt{\epsilon_F - \psi} + \chi\sqrt{\epsilon_h - \psi} & \text{for } \psi \leqslant \epsilon_F \\ \chi\sqrt{\epsilon_h - \psi} & \text{for } \epsilon_F \leqslant \psi \leqslant \epsilon_h \\ 0 & \text{for } \psi \geqslant \epsilon_h\,. \end{cases} \qquad (11)$$

Solving this equation numerically and using the constraints Eqs. (5) and (6) yield the complete solution for the one-particle distribution function. In Fig. 3 we compare the theoretically calculated density and velocity distribution functions to the full N-body simulation. To obtain the distributions in the simulations, the system is evolved for 1000 dynamical times until the stationary state is achieved. To get good statistics the histograms are constructed by binning the particle positions and velocities at four different times. An excellent agreement is found between the theory and the simulations, *without any adjustable parameters*. Note that the agreement is very good for both the virial numbers above and below $\mathcal{R}_0 = 1$. In the same figure we also plot, with the dashed lines, the initial density and the velocity distributions. It is clear that during the process of collisionless relaxation the system moves far from the initial condition. It is important to keep in mind that although the system has relaxed to the stationary state, this state does not correspond to the thermodynamic equilibrium. In particular, the velocity distribution does not have the equilibrium Maxwell-Boltzmann form. This also shows that one needs to take a special care when modeling collisionless system using hydrodynamic-like equations, since there might not be thermodynamic equilibrium even locally.

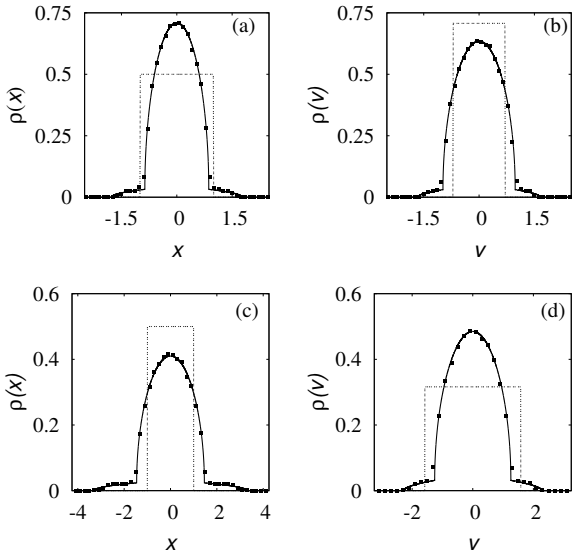

Figure 3. Final position (a) and velocity (b) distributions for initial water-bag with $\mathcal{R}_0 = 0.5$ at t=1000 τ_D. (c) and (d) are the stationary distribution for the initial water-bag with $\mathcal{R}_0 = 2.5$. The dotted lines are the initial distributions.

6 CONCLUSIONS

We have presented a theory which allows us to *a priori* predict the density and the velocity distribution functions for a system of gravitationally interacting sheets. The theory is quantitatively accurate without any fitting parameters. The theory and the simulations show that in the thermodynamic limit this system does not evolve to the usual MB equilibrium. Instead it becomes trapped in a non-ergodic, non-mixing state — once formed, the halo never again equilibrates with the core in the $N \to \infty$ limit.

Although in this paper we have studied only water-bag-like initial distributions, the theory can be easily generalized to more complex functional forms (Teles et al. 2009). The next step in the development of the theory will be to include a specific cosmological model to account for the expansion of the universe. If this can be achieved, the theory might shed new light on the mass distribution in the dark-matter halos.

ACKNOWLEDGMENTS

T.N.T. is grateful to Fernanda Benetti for help with writing the manuscript. The work was partially supported by the CNPq, Fapergs, INCT-FCx, and by the US-AFOSR under the grant FA9550-09-1-0283.

REFERENCES

Barnes E. I., Williams L. L. R., 2011, ApJ, 728, 136
Bindoni D., Secco L., 2007, New Astr. Rev., 52, 1
Binney J., Tremaine S., 2008, Galatic Dynamics, 2nd ed. Princeton Univ. Press, Princeton, NJ
Braun W., Hepp K., 1977, Comm. Math. Phys., 56, 101
Camm G. L., 1950, MNRAS, 110, 305
Campa A., Dauxois T., Ruffo S., 2009, Phys. Rep. 480, 57
Chavanis P.-H., 2006, Physica A, 359, 177
Cuperman S., Goldstein S., Lecar M., 1969, MNRAS, 146, 161
Davidson R. C., Qin H., Physics of Intense charged Particle Beams in High Energy Accelerators (World Scientific, Singapore, 2001)
Gluckstern R. L., 1994, Phys. Rev. Lett., 73, 1247
Gupta S., Mukamel D., 2010, Phys. Rev. Lett., 105, 040602
Hjorth J., Williams L. L. R., 2010, ApJ, 722, 851
Hohl F., Feix M. R., 1967, ApJ, 147, 1164
Hohl F., Campbell J. W., 1968, AJ, 73, 7
Joyce M., Worrakitpoonpon T., 2010a, arXiv Preprint arXiv:1012.5042;
Joyce M., Worrakitpoonpon T., 2010b, J. Stat. Mech., P10012
Joyce M., Sicard F., 2011, MNRAS in press, arXiv:1012.1515
Levin Y., Pakter R., Teles T. N., 2008a, Phys. Rev. Lett., 100, 040604
Levin Y., Pakter R., Rizzato F. B., 2008b, Phys. Rev. E., 78, 021130
Lynden-Bell D., 1967, MNRAS, 136, 101
Mathur S. D., 1990, MNRAS, 243, 529-536
Miller B. N., Rouet J.-L, 2010, J. Stat. Mech., P12028
Navarro J. F., Frenk C. S., White S. D. M., 1995, MNRAS, 275, 270
Navarro J. F., Frenk C. S., White S. D. M., 1996, ApJ, 462, 563
Navarro J. F., Frenk C. S., White S. D. M., 1997, ApJ, 478, 435
Navarro J. F. et al., 2010, MNRAS, 402, 21
Noullez A., Fanelli D., Aurell E., 2003, J. Comp. Phys., 186, 2, 697-703
Padmanabhan T., Phys. Rep., 1990, 188, 5, 285 - 362
Pakter R., Levin Y., 2011, Phys. Rev. Lett., 106, 200603
Reidl C. J. and B. E. N. Miller, 1995, Phys. Rev. E., 51, 884-888
Rybicki G. B., 1971, Ap&SS, 14, 56-72
Saslaw W. C., 2000, The Distribution of the Galaxies: Gravitational Clustering in Cosmology, Cambridge University Press
Shu F. H., 1978, ApJ, 225, 83
Teles T. N., Pakter R., Levin Y., 2009, Appl. Phys. Lett. 95, 173501
Teles T. N., Levin Y., Pakter R., Rizzato F. B., 2010, J. Stat. Mech., P05007
Tsuchiya T. and Gouda N., 1994, Phys. Rev. E, 50, 26072615
Tsuchiya T. and Gouda N., 1996, Phys. Rev. E, 53, 2210-2216
Tsuchiya T. and Gouda N., 2000, Physical Review E, 61, 948
Wangler T. P., Crandall K. R., Ryne R., Wang T. S., 1998, Phys. Rev. ST Accel. Beams, 1, 084201
White S. D. M., Narayan R., 1987, MNRAS, 229, 103
Wright H. L., Miller B. N., and Stein W. E., 1982, Ap&SS, 84, 421
Yamaguchi Y. Y., 2008, Phys. Rev. E, 78, 041114
Yamashiro T., Gouda N. , and Sakagami M.-A, 1992, Progress of Theoretical Physics, 88, 2, 269
Yawn K. R., Miller B. N., 2003, Phys. Rev. E, 68, 056120

APPENDIX A: ENVELOPE EQUATION

We define the "envelope" as $x_e \equiv \sqrt{3 < x^2 >}$. Differentiating twice with respect to time we find,

$$\ddot{x}_e = \frac{3 < x\ddot{x} >}{x_e} + \frac{3 < \dot{x}^2 >}{x_e} - \frac{9 < x\dot{x} >^2}{x_e^3}. \tag{A1}$$

To simplify the first term, we suppose that the mass density oscillations are affine — preserve the uniform mass distribution. In this case,

$$< x\ddot{x} >= - < x\frac{d\psi}{\mathrm{dx}} >= -\frac{1}{2x_e(t)} \int_{-x_e(t)}^{x_e(t)} \frac{x^2}{x_e} \mathrm{dx}\,. \tag{A2}$$

Integrating, we find

$$< x\ddot{x} >= -\frac{x_e(t)}{3}. \tag{A3}$$

The second term of eq. (A1) involves only the mean values which, for short times, should remain close to those obtained using the initial particle distribution function f_0,

$$< \dot{x}^2 >= \frac{1}{2v_m} \int_{-v_m}^{v_m} \dot{x}^2 \mathrm{d\dot{x}} = \frac{v_m^2}{3} \tag{A4}$$

$$< x\dot{x} >= \frac{1}{4\ x_m v_m} \int_{-x_m}^{x_m} x\mathrm{dx} \int_{-v_m}^{v_m} \dot{x}\mathrm{d\dot{x}} = 0$$

Finally the envelope equation reduces to,

$$\ddot{x}_e(t) = \frac{\mathcal{R}_0}{x_e(t)} - 1\ , \tag{A5}$$

where $\mathcal{R}_0 = \frac{2T_0}{U_0} = v_m^2$. Since $x_e(0) = x_m = 1$ if $\mathcal{R}_0 = 1$ then $\ddot{x}_e(t) = 0$, and the system does not develop macroscopic collective oscillations.